

# Superhydrophobic Alkanethiol-Coated Microsubmarines for Effective Removal of Oil

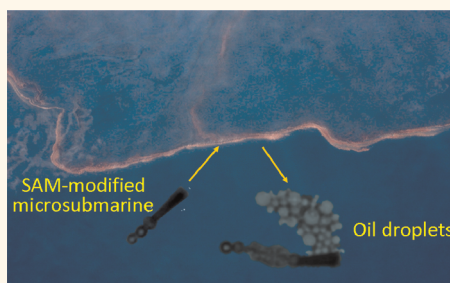
Maria Guix,<sup>†,\*,‡</sup> Jahir Orozco,<sup>†,‡</sup> Miguel García,<sup>†,§,‡</sup> Wei Gao,<sup>†</sup> Sirilak Sattayasamitsathit,<sup>†</sup> Arben Merkoçi,<sup>‡</sup> Alberto Escarpa,<sup>§</sup> and Joseph Wang<sup>†,\*</sup>

<sup>†</sup>Department of Nanoengineering, University of California—San Diego, La Jolla, California 92093, United States, <sup>‡</sup>ICREA & Catalan Institute of Nanotechnology, Campus University Autònoma of Barcelona, E-08193 Bellaterra, Barcelona, Spain, and <sup>§</sup>Department of Analytical Chemistry and Chemical Engineering, University of Alcalá, E-28871 Alcalá de Henares, Madrid, Spain. <sup>‡</sup>These authors have contributed equally to this work.

Self-propelled catalytic nanomotors, capable of converting energy into movement and forces,<sup>1–6</sup> have shown considerable promise for diverse practical applications. Particularly attractive are tubular microengines owing to their efficient bubble-induced propulsion in complex biological media and high ionic-strength environments.<sup>4,7,8</sup> Such chemically powered nanomotors have been commonly prepared by top-down photolithography, e-beam evaporation, and stress-assisted rolling of functional nanomembranes into conical microtubes.<sup>5</sup> Alternatively, a simplified membrane-template electrodeposition protocol can be used for mass production of high-performance catalytic microtubular engines.<sup>9,10</sup> The resulting microengines are smaller in size ( $\sim 8 \mu\text{m}$  long), require low fuel concentrations (down to 0.2%  $\text{H}_2\text{O}_2$ ), and move at an ultrafast speed (over 1400 body lengths/s). These template-fabricated microtubes commonly consist of a polymer/Pt bilayer and require additional Ni and Au layers for their magnetic guidance and facile functionalization (e.g., with receptors), respectively. A judicious modification of the outer Au surface by molecular bioreceptors, e.g., DNA probes,<sup>11</sup> aptamers,<sup>12</sup> antibodies,<sup>13</sup> or lectins,<sup>14</sup> has thus been shown useful for diverse target-isolation sensing applications. Considerable efforts have also been devoted toward the use of catalytic nanomotors for targeted drug delivery.<sup>15</sup>

In this paper we demonstrate the first example of using functionalized nanomachines toward environmental remediation of contaminated water. In particular, we illustrate how the deliberate modification of the rough outer surface of microengines with highly hydrophobic long-chain self-assembled alkanethiol monolayers offers

## ABSTRACT



We demonstrate the use of artificial nanomachines for effective interaction, capture, transport, and removal of oil droplets. The simple nanomachine-enabled oil collection method is based on modifying microtube engines with a superhydrophobic layer able to adsorb oil by means of its strong adhesion to a long chain of self-assembled monolayers (SAMs) of alkanethiols created on the rough gold outer surface of the device. The resultant SAM-coated Au/Ni/PEDOT/Pt microsubmarine displays continuous interaction with large oil droplets and is capable of loading and transporting multiple small oil droplets. The influence of the alkanethiol chain length, polarity, and head functional group and hence of the surface hydrophobicity upon the oil–nanomotor interaction and the propulsion is examined. No such oil–motor interactions were observed in control experiments involving both unmodified microengines and microengines coated with SAM layers containing a polar terminal group. These results demonstrate that such SAM-Au/Ni/PEDOT/Pt micromachines can be useful for a facile, rapid, and efficient collection of oils in water samples, which can be potentially exploited for other water–oil separation systems. The integration of oil-sorption properties into self-propelled microengines holds great promise for the remediation of oil-contaminated water samples and for the isolation of other hydrophobic targets, such as drugs.

**KEYWORDS:** superhydrophobic · microsubmarine · nanomachine · self-assembled monolayer · environmental remediation · oil collection · liquid–liquid interface · self-propulsion

considerable promise for the capture, transport, and removal of oil droplets from water samples. Oil is a major source of ocean pollution and groundwater contamination. The presence of oils in wastewaters as a product of various manufacturing processes is common in different industries. Furthermore, episodes of major water pollution, caused by oil spillage, result in the release

\* Address correspondence to josephwang@ucsd.edu.

Received for review March 16, 2012 and accepted April 5, 2012.

Published online April 05, 2012  
10.1021/nn301175b

© 2012 American Chemical Society

of millions of tons each year. For example, the 1989 *Exxon Valdez* and 2010 *Deepwater Horizon* incidents spilled millions of gallons of crude oil.<sup>16,17</sup> The removal of oils and organic solvents from contaminated water is thus of considerable importance for minimizing the environmental impact of these pollutants.

Substantial efforts have thus been devoted to develop effective tools toward the remediation and cleanup of oil spills. Although oils in wastewater plants are mostly removed by a mechanical separation, other methods have been proposed to address related pollution episodes.<sup>18,19</sup> However, most of these methods lack the desired selectivity and efficiency and are not cost-effective or environmentally friendly. Accordingly, the development of new highly effective oil–water separation methods is highly desired.

Different synthetic and natural materials have been proposed as possible sorbents for oil removal. Surfaces with superhydrophobic properties have recently attracted particular interest for oil–water separation owing to their high efficiency and selectivity,<sup>18–22</sup> although their high cost, complex preparation processes, and scalability issues have hindered their practical applications.<sup>16</sup> These hydrophobic surfaces tend to repel water while strongly interact with non-polar or oily liquids, which firmly adhere to textured interfaces.<sup>21</sup> Both the micronano-hierarchical texture and the chemical composition are essential for promoting the superhydrophobic character necessary for effective oil removal. The surface polarity and roughness are thus expected to influence the extent of the oil–surface interaction.<sup>23,24</sup> Self-assembled monolayers (SAMs), formed by the spontaneous and strong chemisorption of alkanethiols at gold or silver surfaces, have been particularly useful for transforming these surfaces into superhydrophobic interfaces.<sup>24</sup> Guo *et al.*<sup>25</sup> reported that ZnO hydrophilic surfaces become superhydrophobic after exposure to an octadecanethiol solution. Tailoring the length of the alkanethiol chain has allowed the control of the surface polarity and hence tuning the partition of hydrophobic drugs.<sup>26</sup> The choice of the ending functional group is also vital for tailoring the polarity of the SAMs. For example, water contact angle studies reveal that methyl-terminated SAMs lead to hydrophobic surfaces, while hydroxyl-terminated ones provide wettable surfaces.<sup>27</sup> However, there are no reports of integrating these oil-sorption properties into self-propelled microengines and using such superhydrophobic nanomotors to facilitate the capture, transport, and separation of oil droplets. Autonomously moving synthetic nanomotors have recently been employed for the pick-up and transport of diverse payloads, ranging from cancer cells to drug-loaded polymeric spheres,<sup>12,14</sup> but not in connection to the isolation of oily contaminants.

The method herein presented is based on the creation of a SAM-modified microtubular engine able to

strongly interact with oily liquids *via* adhesion and permeation onto its long alkanethiol coating. As illustrated in Figure 1, the new catalytic microsubmarine is template-prepared by electroplating poly(3,4-ethylenedioxythiophene) (PEDOT)/Pt bilayer followed by e-beam deposition of Ni/Au and subsequent functionalization with the SAM. In particular, dodecanethiol-coated Au/Ni/PEDOT/Pt microsubmarines are shown in the following sections to offer an effective capture and transport of oil droplets from aqueous media. The influence of the alkanethiol chain length upon the oil–nanomotor interaction and the collection efficiency has been examined using SAMs of different chain lengths, *i.e.*, hexanethiol (C6), dodecanethiol (C12), and octadecanethiol (C18). The optimal C12 superhydrophobic SAM-coated microsubmarine has shown a strong prolonged interaction with large oil droplets (attached to the glass-slide surface) along with the effective pickup and transport of multiple small oil droplets present in an oil-contaminated water sample. Unmodified microengines did not show such affinity to oil droplets. These results demonstrate that SAM-functionalized microsubmarines can be useful for facile, rapid, and highly efficient collection of oils in water samples. This high oil-adsorption ability indicates considerable potential for environmental remediation of oil-contaminated water samples and other contaminated water systems.

## RESULTS

The fabrication of the oil-sorption hydrophobic microsubmarines, depicted in Figure 1, involves a template-based electrodeposition of a PEDOT/Pt bilayer microtube and e-beam vapor deposition of the Ni and Au outer layers, essential for the magnetic navigation control and surface functionalization, respectively. As illustrated in Figure 1A(d), such functionalization involves the formation of a superhydrophobic layer by self-assembly of long alkanethiol chains on the rough outer gold surface. A SEM image of the unmodified microengine (Figure 1B) indicates a rough surface, characteristic of nitrate-doped PEDOT films.<sup>10</sup> The template fabrication process results in 8  $\mu\text{m}$  long microtubes that are substantially smaller than common rolled-up tubular microengines.<sup>28</sup> The relatively similar dimensions of microsubmarine and oil droplets (which range from  $\sim 1$  to  $\sim 100 \mu\text{m}$ , depending on the emulsion composition) permit convenient real-time optical visualization of the oil–microengine interaction. Similar to recently developed PANI/Pt microengines,<sup>9</sup> the new template-prepared PEDOT/Pt microtubes were propelled efficiently in different media *via* the expulsion of oxygen bubbles generated from the catalytic oxidation of hydrogen peroxide fuel at their inner Pt layer.<sup>10</sup> Several factors, such as additional Ni and Au layers, influence the microengine speed.

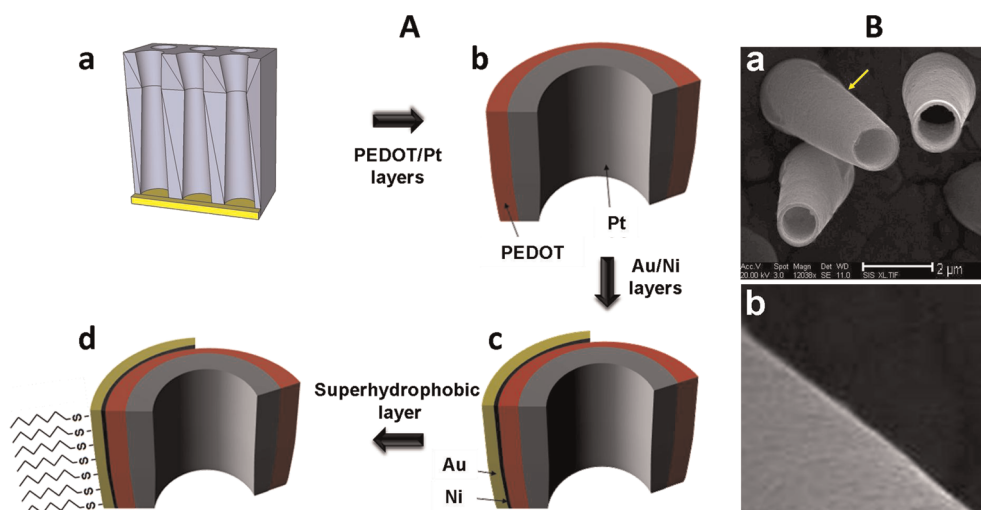


**Figure 1.** Fabrication and modification of the SAM-Au/Ni/PEDOT/Pt micromotors for environmental remediation. (A) A Cyclopore polycarbonate membrane is used as a template (a), PEDOT and Pt layers are electroplated into the template (b), Au and Ni layers are sputtered by e-beam (c), and a superhydrophobic layer is formed on the microsubmarine surface by incubation in a 0.5 mM *n*-dodecanethiol ethanolic solution (d). (B) SEM image of the resulting PEDOT/Pt microsubmarine (a) with a zoom-in of the zone highlighted with a yellow arrow (b).

**TABLE 1.** Average Speed of the Microsubmarine upon Each Step Involved in the Fabrication Process and Pick-up of Oil Droplets

microsubmarine step	speed, $\mu\text{m/s}$
PEDOT/Pt	420
Au/Ni/PEDOT/Pt	200
SAM/Au/Ni/PEDOT/Pt	105
SAM/Au/Ni/PEDOT/Pt/few (1–5) droplets	20–50
SAM/Au/Ni/PEDOT/Pt/numerous droplets	10–20

For example, and as expected for polymer/Pt micro-engines,<sup>14</sup> the fast speed of the PEDOT/Pt microengines ( $\sim 420 \mu\text{m/s}$  average) is reduced by up to 50% after the e-beam deposition of the outer Ni/Au layers.

The resulting Au/Ni/PEDOT/Pt microsubmarines were then immersed in a 0.5 mM dodecanethiol ethanolic solution for 30 min to form the hydrophobic monolayers on the outer gold surface, as illustrated in Figure 1D (see Methods Section in the Supporting Information for additional details). Such surface modification of the Au/Ni/PEDOT/Pt microsubmarine resulted in an additional  $\sim 50\%$  speed reduction, reflecting the partial blocking of the inner Pt catalytic layer.<sup>29</sup> However, the reduced speed is sufficient for transporting large cargoes in a manner analogous to our previously reported Au/Ni/PANI/Pt microengines.<sup>14</sup> Table 1 summarizes the changes in the microsubmarines' speed due to each different step involved in the fabrication process.

Figure 2A and Supporting Video S1A (right side) show the Au/Ni/PEDOT/Pt micromotor approaching, contacting, and spinning around a stained olive oil drop firmly attached to a glass slide (see additional details in the Supporting Information). The strong interaction between the SAM-modified microsubmarine and an oil

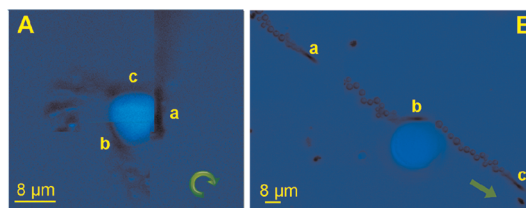


**Figure 2.** SAM-modified (A) and unmodified (B) microsubmarines in the presence of a stained olive oil droplet (attached to a glass slide). Images, taken from video 1, show (in a single overlaid image) the following sequential steps: approaching, contacting, and spinning around (A, a–c) the droplet and approaching, contacting, and leaving (B, a–c) the oil droplet, respectively. Fuel conditions (final concentration): 0.4% NaCh and 10%  $\text{H}_2\text{O}_2$ . Arrows indicate the microsubmarine trajectory.

droplet results in a continuous spinning of the modified engine around the droplet with an accelerated speed ranging up to  $200 \mu\text{m/s}$ . It should be pointed out that such continuous high-speed spinning is observed even after a prolonged 20 min period. These data also confirm that the hydrogen peroxide fuel and the sodium cholate (NaCh) surfactant, essential for the microsubmarine movement, do not compromise its interaction with the oil droplet or the integrity of the SAM. In contrast, no such interaction is observed using an unmodified microsubmarine (Figure 2B and Supporting Video S1 left side). This bare Au/Ni/PEDOT/Pt micromotor moves rapidly, while approaching, contacting, and bypassing the droplet. Supporting Video S1B shows different unmodified microsubmarines contacting, but not interacting, with olive oil droplets of different sizes (from 5 to  $25 \mu\text{m}$ ; attached to a glass slide).

Efficient capture and transport of oil droplets has been observed when the modified microsubmarine navigates in contaminated water samples containing

small “free-floating” oil droplets. Figure 3 and Supporting Video S2 illustrate the capture and transport of multiple small olive oil droplets by the SAM-modified microsubmarine. The longer the navigation time, the more oil droplets are collected and confined onto the surface of the self-propelled micromotor. While around 5 droplets ( $1.7 \pm 0.4 \mu\text{m}$  size) are captured and transported in Figure 3A (and starting Supporting Video S2) after a 12 s navigation, around 40 droplets are attached to the motor surface following 80 s (Figure 3A(d) and ending Supporting Video S2). These observations demonstrate that these SAM-modified microengines provide high towing force for transporting efficiently approximately 10-fold their volume and indicate considerable potential for oil removal applications. As expected from the increased drag force (Stokes's law),<sup>30</sup> the speed of the micromachine decreases upon increasing the cargo size (*i.e.*, number of captured droplets). This is illustrated in Figure 3B, which displays the dependence of the microsubmarine speed on the number of transported oil droplets. The speed rapidly decreases from 26 to  $12 \mu\text{m/s}$  upon increasing the number of droplets from 7 to 30 and then more slowly to  $11 \mu\text{m/s}$  for 43 droplets. As common for nanomotor-based cargo pickup, the optimal motor speed will provide a trade-off between sufficient contact time and large contact rate.<sup>31,32</sup>

Particularly attractive is the ability to tailor the polarity of the microsubmarine surface *via* a judicious choice of the chain length of the *n*-alkanethiol coating and hence their capture and transport properties. Chain length, head groups, preparation time, and other conditions (*e.g.*, temperature) give rise to different SAM packing densities, configurations, and polarity.<sup>33</sup> The influence of the alkanethiol chain length on the oil–nanomotor interaction was thus examined by modifying the microengine with SAMs of different alkanethiol lengths (C6, C12, and C18). A considerable difference in the microsubmarine–oil droplet interaction was observed using C6 and C12 SAM-coated microsubmarines. Notice, for example, the strong microsubmarine–oil interaction of the C12-modified microengine spinning around a large olive oil droplet (Figure 2B and Supporting Video S1A, right part) compared to the weaker interaction experienced by the C6-modified motor, where no spinning around the droplet is observed (Supporting Figure 1A and Supporting Video S3). Similarly, Supporting Information Figure 2 and Video S4 illustrate the higher number of captured oil droplets using the C12 SAM modification (C) compared to the lower number of droplets attached to the C6-modified motor (B) and to the absence of captured droplets using the unmodified microsubmarine (A). These results are consistent with the different surface wettability properties observed in contact angle studies of *n*-alkanethiols of different lengths.<sup>33,34</sup> On the basis of the higher hydrophobic character of long-chain thiols, C18 SAM-coated microsubmarines are

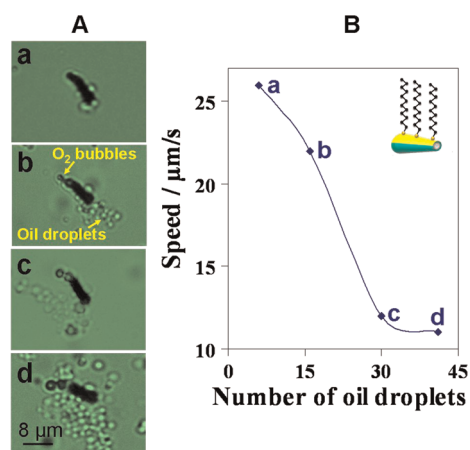


**Figure 3.** Dodecanethiol (C12-SAM)-modified microsubmarine carrying floating olive oil droplets. (A) Images a–d were taken from video 2 after navigating in the water–oil (10% fuel) solution for 5, 12, 66, and 80 s, respectively (conditions, as in Figure 2). (B) Dependence of the microsubmarine speed upon the number of cargos (olive oil droplets). Inset: Cartoon of the dodecanethiol-modified microsubmarine.

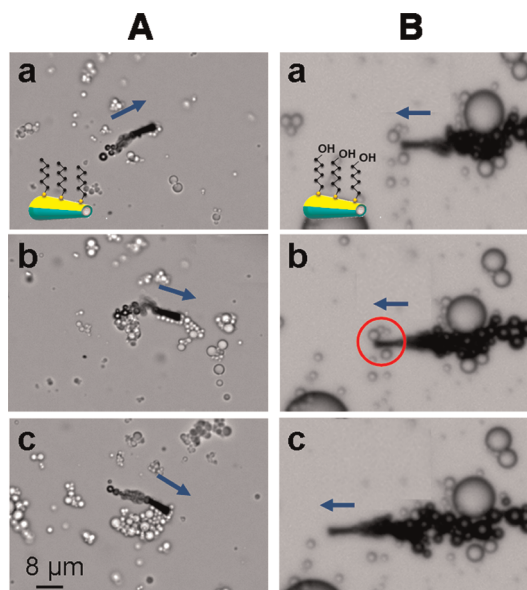


**Figure 4.** C6-SAM-modified microsubmarines with different head functional groups interacting with small olive oil droplets. Hexanethiol-modified microsubmarines are able to confine a payload of multiple oil droplets (A) (a, b, and c, time-lapse images at different navigation times: 11, 50, and 73 s (for A) and 6.57, 6.66, and 6.71 s (for B)). The corresponding mercaptohexanol-modified counterparts (B) are not able to pick up such droplets (a, b, and c images correspond to approaching, contacting, and leaving the droplets). A(a) and B(a) insets: cartoons of the respective SAM-modified microsubmarines. Arrows indicate the direction of the microsubmarine movement.

expected to offer higher oil-adsorption capabilities. However, such C18 SAM-modified microsubmarines hardly move owing to greater blocking of the inner Pt catalytic layer expected in the presence of longer alkanethiols.<sup>29</sup> Selective modification using alkane isonitriles<sup>35</sup> may be used to minimize the Pt blocking by the alkanethiol SAM, thus retaining microengine speed.

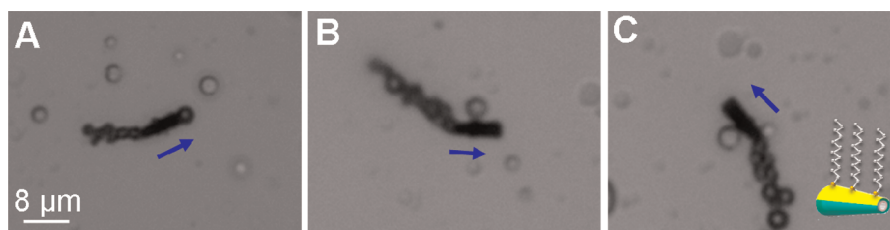


**Figure 5.** SAM-modified microsubmarine carrying floating droplets of motor oil in a fuel-enhanced oil-contaminated water sample. Images taken from video 6 after 78 s navigation in the fuel-enhanced solution (conditions, as in Figure 2). (A, B, C) Time-lapse images showing the microsubmarine approaching, contacting, and carrying the droplets, respectively. Inset: Cartoon of the dodecanethiol-modified microsubmarine. Arrows indicate the direction of the microsubmarine movement.

The influence of the SAM headgroup and hence surface polarity on the microsubmarines–oil interaction was examined by comparing the behavior of microengines coated with C6 SAM containing methyl and hydroxyl terminal groups using different time scales. Figure 4A(a–c) and Supporting Video S5 illustrate small droplets attached to the hexanethiol-modified microsubmarine upon navigating in the sample. In contrast, and as expected from wettability measurements using hydroxyl-terminated SAM,<sup>27</sup> the mercaptohexanol-modified microsubmarines do not interact with the large or small olive oil droplets upon rapidly contacting them (Supporting Figure 1B and Figure 4B, a–c). It is remarkable that even prolonged navigation of the mercaptohexanol-modified microsubmarines does not lead to any capture of the oil droplets. Clearly, and as expected,<sup>27</sup> the polarity of the head functional group strongly influences the interaction between the modified microsubmarines and the oil droplets and represents another key consideration (besides the chain length) when modifying the outer microengine surface.

Toward a practical utility of this new microsubmarine approach, we examined the ability of the dodecanethiol-modified microsubmarine to collect and transport motor oil in an oil-contaminated water sample. Figure 5 and the corresponding Supporting Video S6 clearly illustrate that the SAM-coated microsubmarines display an “on the fly” capture upon contacting the small droplets of motor oil that are floating in the contaminated water sample. These results demonstrate the potential of the superhydrophobic-modified microsubmarines for facile, rapid, and highly efficient collection of oils in oil-contaminated water samples.

## CONCLUSIONS

We have presented the first example of using artificial nano/microscale machines for environmental remediation applications and specifically the tailoring of the surface of such self-propelled machines to interact

strongly with oily liquids. The new SAM-Au/Ni/PEDOT/Pt micromotors thus offer a facile, rapid, and highly efficient collection and transport of oil droplets in aqueous environments through the interaction with the hydrophobic alkanethiol monolayer coating. Comparison of different alkanethiol modifiers indicates that the dodecanethiol (C12-SAM)-modified microsubmarines offer the most favorable performance in terms of oil recovery and propulsion. Such high oil-adsorption ability indicates considerable promise for the cleanup of contaminated water samples. The extent of the micromotor–oil interaction and the collection efficiency can be tuned by controlling the surface hydrophobicity through the use of different chain lengths and head functional groups. The new microsubmarine capability was demonstrated either by a strong interaction between the modified nanomotor and large oil droplets (attached to a glass slide) or by the collection and transport of multiple free-floating small olive oil and motor oil droplets present in a contaminated water sample. These micromotor–oil interactions can be exploited in the suitable final disposition of oily wastes (or other organic solvents) by collecting them in a controlled fashion within a certain spatially separated zone. Simultaneous parallel movement of multiple SAM-modified microsubmarines holds promise for improving the efficiency of oil-removal processes. Practical large-scale oil cleaning operations would require the use of motors propelled by their own natural environment<sup>36,37</sup> or driven by an external (magnetic or electrical) control.<sup>38,39</sup> The new superhydrophobic microswimmers offer also considerable promise for the isolation of hydrophobic molecules, *e.g.*, drugs, or for transferring target analytes between liquid–liquid immiscible interfaces, and hence great potential for diverse analytical microsystems. Multifunctional coatings of mixed (or multi) layers, coupling the preferential partition of hydrophobic compounds into the SAMs with additional functions (*e.g.*, biocatalysis), could lead to additional advantages toward on-the-fly “capture and destroy” operations.

## EXPERIMENTAL SECTION

**Synthesis of Multilayer Microsubmarines.** The multilayer microtubes were prepared using a common template-directed

electrodeposition protocol.<sup>9,10</sup> A cyclopore polycarbonate membrane, containing 2  $\mu\text{m}$  maximum diameter conical-shaped micropores (Catalog No. 7060-2511; Whatman, Maidstone, U.K.), was employed as the template. A 75 nm gold film was

first sputtered on one side of the porous membrane to serve as working electrode using the Denton Discovery 18. The sputter was performed at room temperature under vacuum of  $5 \times 10^{-6}$  Torr, dc power of 200 W, and Ar flow of 3.1 mT. Rotation speed is 65  $\mu\text{m/s}$ . Sputter time is 90 s. A Pt wire and an Ag/AgCl with 3 M KCl were used as counter and reference electrodes, respectively. The membrane was then assembled in a plating cell with an aluminum foil serving as contact. Poly(3,4-ethylenedioxythiophene) microtubes were prepared by modifying the previously described method.<sup>10</sup> Briefly, PEDOT microtubes were electropolymerized up to 0.1 C at +0.80 V from a plating solution containing 15 mM EDOT monomer, 50 mM SDS, and 7.5 mM  $\text{KNO}_3$ , all of them prepared from Sigma-Aldrich reagents. The inner Pt tube was deposited galvanostatically at  $-2$  mA for 600 s from a commercial platinum plating solution (Platinum RTP; Technic Inc., Anaheim, CA, USA). The sputtered gold layer was completely removed by mechanical hand polishing with 3–4  $\mu\text{m}$  alumina slurry. Incomplete removal will result in bubbles emerging from the smaller opening of the microengine (yet without compromising its performance). Finally, microengines were collected by centrifugation at 6000 rpm for 3 min and washed repeatedly with methylene chloride, followed by ethanol and ultrapure water (18.2 M $\Omega$  cm), three times of each, with a 3 min centrifugation following each wash. The microtube suspension was evaporated onto glass slides before the sequential deposition of 10 nm of Ti (adhesion layer), 15 nm of Ni (magnetic layer), and 15 nm of Au (functionalization layer) over the microtubes by using electron beam deposition. These additional steps provide the necessary magnetic directional control and the appropriate gold surface for the later modification with self-assembled monolayers.

**Microsubmarine Modification.** The external gold surface of the microsubmarines was modified by immersion in 0.5 mM dodecanethiol in absolute ethanol (from Sigma-Aldrich), after which the resulting monolayer-modified microsubmarines were washed with Milli-Q water and isolated by centrifugation at 6000 rpm during 4 min. All experiments were carried out at room temperature. Study of the chemical structure effect, e.g., length chain and terminal groups, on the speed was performed with different thiols, including hexanethiol, mercaptohexanol, dodecanethiol, and octadecanethiol, all received from Sigma-Aldrich and dissolved in ethanol. Bare microsubmarines without the monolayer were also used as control experiments.

**Equipment.** Template electrochemical deposition of microtubes was carried out with a CHI 661D potentiostat (CH Instruments, Austin, TX, USA). An inverted optical microscope (Nikon Eclipse Instrument Inc. Ti-S/L100), coupled with a 40 $\times$  objective, using a Hamamatsu digital camera C11440 and NIS-Elements AR 3.2. software, was used for capturing movies at a frame rate of 20 frames per second. The speed of the microengines was tracked using a NIS-Elements tracking module, and the results were statistically analyzed using Origin software.

**Experimental Procedure.** In order to self-propel the catalytic microsubmarines around different oil droplets or capture such droplets, an emulsion containing Milli-Q water/oil sample/6% sodium cholate (NaCh) (2:2:1) was first prepared. A known volume of this solution was spread on a glass slide, and an equal volume of a solution containing the microsubmarines and the same volume of hydrogen peroxide was added to get a final concentration of 0.4% NaCh and 10%  $\text{H}_2\text{O}_2$ . Microsubmarines approach the oil droplets either to spin them around for several minutes (up to 20) or to pick up and carry them. Experiments were performed using olive and motor oils dispersed in Milli-Q water. Initial experiments were carried out with Nile-red-stained olive oil for improved visualization under microscopy. However, the dye was not used in most subsequent experiments, as the water–oil interface was sufficiently distinguishable without such staining.

**Conflict of Interest:** The authors declare no competing financial interest.

**Acknowledgment.** This work was supported by the National Science Foundation (NSF Award Number CBET 0853375) and NATO Science for Peace and Security Program (SfP 983807). M. Guix acknowledges the support from Spanish MICINN. J. Orozco

and M. García are thankful for funding from a Beatrice de Pinós postdoctoral fellowship (Government of Catalonia) and University of Alcalá (Madrid), respectively.

**Supporting Information Available:** Supporting videos and detailed methods. This material is available free of charge via the Internet at <http://pubs.acs.org>.

## REFERENCES AND NOTES

- Paxton, W. F.; Kistler, K. C.; Olmeda, C. C.; Sen, A., St.; Angelo, S. K.; Cao, Y.; Mallouk, T. E.; Lammert, P. E.; Crespi, V. H. Catalytic Nanomotors: Autonomous Movement of Striped Nanorods. *J. Am. Chem. Soc.* **2004**, *126*, 13424–13431.
- Ozin, G. A.; Manners, I.; Fournier-Bidoz, S.; Arsenault, A. Dream Nanomachines. *Adv. Mater.* **2005**, *17*, 3011–3018.
- Fournier-Bidoz, S.; Arsenault, A. C.; Manners, I.; Ozin, G. A. Synthetic Self-Propelled Nanorotors. *Chem. Commun.* **2005**, *41*, 441–443.
- Wang, J. Can Man-Made Nanomachines Compete with Nature Biomotors?. *ACS Nano* **2009**, *3*, 4–9.
- Pumera, M. Electrochemically Powered Self-Propelled Electrophoretic Nanosubmarines. *Nanoscale* **2010**, *2*, 1643–1649.
- Campuzano, S.; Kagan, D.; Orozco, J.; Wang, J. Motion-Driven Sensing and Biosensing Using Electrochemically Propelled Nanomotors. *Analyst* **2011**, *136*, 4621–4630.
- Mei, Y.; Solovev, A. A.; Sanchez, S.; Schmidt, O. G. Rolled-up Nanotech on Polymers: From Basic Perception to Self-Propelled Catalytic Microengines. *Chem. Soc. Rev.* **2011**, *40*, 2109–2119.
- Huang, G.; Wang, J.; Mei, Y. Material Considerations and Locomotive Capability in Catalytic Tubular Microengines. *J. Mater. Chem.* **2012**, *22*, 6519–6525.
- Gao, W.; Sattayasamitsathit, S.; Orozco, J.; Wang, J. Highly Efficient Catalytic Microengines: Template Electro-synthesis of Polyaniline-Platinum Microtubes. *J. Am. Chem. Soc.* **2011**, *133*, 11862–11864.
- Gao, W.; Sattayasamitsathit, S.; Uygun, A.; Pei, A.; Ponedal, A.; Wang, J. Polymer-Based Tubular Microbots: Role of Composition and Preparation. *Nanoscale* **2012**, *4*, 2447–2453.
- Kagan, D.; Campuzano, S.; Balasubramanian, S.; Kuralay, F.; Flechsig, G.; Wang, J. Functionalized Micromachines for Selective and Rapid Isolation of Nucleic Acid Targets from Complex Samples. *Nano Lett.* **2011**, *11*, 2083–2087.
- Orozco, J.; Campuzano, S.; Kagan, D.; Zhou, M.; Gao, W.; Wang, J. Dynamic Isolation and Unloading of Target Proteins by Aptamer-Modified Microtransporters. *Anal. Chem.* **2011**, *83*, 7962–7969.
- Balasubramanian, S.; Kagan, D.; Hu, C. J.; Campuzano, S.; Lobo-Castaño, M. J.; Lim, N.; Kang, D. Y.; Zimmerman, M.; Zhang, L.; Wang, J. Micromachine-Enabled Capture and Isolation of Cancer Cells in Complex Media. *Angew. Chem. Int. Ed.* **2011**, *50*, 4161–4164.
- Campuzano, S.; Orozco, J.; Kagan, D.; Guix, M.; Gao, W.; Sattayasamitsathit, S.; Claussen, J. C.; Merkoçi, A.; Wang, J. Bacterial Isolation by Lectin-Modified Microengines. *Nano Lett.* **2012**, *12*, 396–401.
- Kagan, D.; Laocharoensuk, R.; Zimmerman, M.; Clawson, C.; Balasubramanian, S.; Kang, D.; Bishop, D.; Sattayasamitsathit, S.; Zhang, L.; Wang, J. Rapid Delivery of Drug Carriers Propelled and Navigated by Catalytic Nanoshuttles. *Small* **2010**, *6*, 2741–2747.
- Biswas, S.; Chaudhari, S. K.; Mukherji, S. Microbial Uptake of Diesel Oil Sorbed on Soil and Oil Spill Clean-up Sorbents. *J. Chem. Technol. Biotechnol.* **2005**, *80*, 587–593.
- Machlis, G. E.; McNutt, M. K. Scenario-Building for the Deepwater Horizon Oil Spill. *Science* **2010**, *329*, 1018–1019.
- Zhu, Q.; Pan, Q.; Liu, F. Facile Removal and Collection of Oils from Water Surfaces through Superhydrophobic and Superoleophilic Sponges. *J. Phys. Chem. C* **2011**, *115*, 17464–17470.
- Cheng, M.; Gao, Y.; Guo, X.; Shi, Z.; Chen, J. F.; Shi, F. A Functionally Integrated Device for Effective and Facile Oil Spill Cleanup. *Langmuir* **2011**, *27*, 7371–7375.

20. Yao, X.; Song, Y.; Jiang, L. Applications of Bio-Inspired Special Wettable Surfaces. *Adv. Mater.* **2011**, *23*, 719–734.
21. McHale, G.; Shirtcliffe, N. J.; Aqil, S.; Perry, C. C.; Newton, M. I. Topography Driven Spreading. *Phys. Rev. Lett.* **2004**, *93*, 036102.
22. Zhang, J.; Pu, G.; Severtson, S. J. Fabrication of Zinc Oxide/Polydimethylsiloxane Composite Surfaces Demonstrating Oil-Fouling-Resistant Superhydrophobicity. *ACS Appl. Mater. Interfaces* **2010**, *2*, 2880–2883.
23. Shirtcliffe, N.; McHale, G.; Newton, M. I.; Chabrol, G.; Perry, C. C. Dual-Scale Roughness Produces Usually Water-Repellent Surfaces. *Adv. Mater.* **2004**, *16*, 1929–1932.
24. Fragoso, A.; Laboria, N.; Latta, D.; Sullivan, C. K. O. Electron Permeable Self-Assembled Monolayers of Dithiolated Aromatic Scaffolds on Gold for Biosensor Applications. *Anal. Chem.* **2008**, *80*, 2556–2563.
25. Guo, M.; Diao, P.; Cai, S. Highly Hydrophilic and Superhydrophobic ZnO Nanorod Array Films. *Thin Solid Films* **2007**, *515*, 7162–7166.
26. Wang, J.; Wu, H.; Angnes, L. On-Line Monitoring of Hydrophobic Compounds at Self-Assembled Monolayer Modified Amperometric Flow Detectors. *Anal. Chem.* **1993**, *65*, 1893–1896.
27. Faucheux, N.; Schweiss, R.; Lutzow, K.; Werner, C.; Groth, T. Self-Assembled Monolayers with Different Terminating Groups as Model Substrates for Cell Adhesion Studies. *Biomaterials* **2004**, *25*, 2721–2730.
28. Sanchez, S.; Solovev, A. A.; Schulze, S.; Schmidt, O. G. Controlled Manipulation of Multiple Cells using Catalytic Microbots. *Chem. Commun.* **2011**, *47*, 698–700.
29. Florida, M. A.; Rubert, A. A.; Benitez, G. A.; Fonticelli, M. H.; Carrasco, J.; Carro, P.; Salvarezza, R. C. Alkanethiol Adsorption on Platinum: Chain Length Effects on the Quality of Self-Assembled Monolayers. *J. Phys. Chem. C* **2011**, *115*, 17788–17798.
30. Wang, J. Cargo-Towing Synthetic Nanomachines: Towards Active Transport in Microchip Devices. *Lab Chip* **2012**, DOI: 10.1039/C2LC00003B.
31. Katira, P.; Hess, H. Two-Stage Capture Employing Active Transport Enables Sensitive and Fast Biosensors. *Nano Lett.* **2010**, *10*, 567–572.
32. Agarwal, A.; Katira, P.; Hess, H. Millisecond Curing Time of a Molecular Adhesive Causes Velocity-Dependent Cargo-Loading of Molecular Shuttles. *Nano Lett.* **2009**, *9*, 1170–1175.
33. Mendoza, S. M.; Arfaoui, I.; Zanarini, S.; Paolucci, F.; Rudolf, P. Improvements in the Characterization of the Crystalline Structure of Acid-Terminated Alkanethiol Self-Assembled Monolayers on Au(111). *Langmuir* **2007**, *23*, 582–588.
34. Offord, D. A.; John, C. M.; Linford, M. R.; Griffin, J. H. Contact Angle Goniometry, Ellipsometry, and Time-of-Flight Secondary Ion Mass Spectrometry of Gold Supported, Mixed Self-Assembled Monolayers Formed from Alkyl Mercaptans. *Langmuir* **1994**, *10*, 883–889.
35. Lee, T. R.; Laibinis, P. E.; Folkers, J. P.; Whitesides, G. M. Heterogeneous Catalysis on Platinum and Self-Assembled Monolayers on Metal and Metal Oxide Surfaces (Note a). *Pure Appl. Chem.* **1991**, *63*, 821–828.
36. Gao, W.; Uygun, A.; Wang, J. Hydrogen-Bubble-Propelled Zinc-Based Microrockets in Strongly Acidic Media. *J. Am. Chem. Soc.* **2012**, *134*, 897–900.
37. Zhao, G.; Seah, T. H.; Pumera, M. External-Energy-Independent Polymer Capsule Motors and Their Cooperative Behaviors. *Chem. Eur. J.* **2011**, *17*, 12020–12026.
38. Zhang, L.; Abbott, J. J.; Dong, L.; Peyer, K. E.; Kratochvil, B. E.; Zhang, H.; Bergeles, C.; Nelson, B. J. Characterizing the Swimming Properties of Artificial Bacterial Flagella. *Nano Lett.* **2009**, *9*, 3663–3667.
39. Loget, G.; Kuhn, A. Electric Field-Induced Chemical Locomotion of Conducting Objects. *Nat. Commun.* **2011**, *2*, 535, DOI: 10.1038/ncomms1550.